

# In-situ frequency tuning of photons stored in a high Q microwave cavity.

M. Sandberg,\* C. M. Wilson, F. Persson, G. Johansson, V. Shumeiko, and P. Delsing  
*Department of Microtechnology and Nanoscience (MC2),  
Chalmers University of Technology, SE-412 96 Göteborg, Sweden*

T. Duty

*School of Physical Sciences, The University of Queensland, Brisbane QLD 4072 Australia.*

(Dated: October 31, 2018)

Photons are fundamental excitations of the electromagnetic field and can be captured in cavities. For a given cavity with a certain size, the fundamental mode has a fixed frequency  $f$  which gives the photons a specific "colour". The cavity also has a typical lifetime  $\tau$ , which results in a finite linewidth  $\delta f$ . If the size of the cavity is changed fast compared to  $\tau$ , and so that the frequency change  $\Delta f \gg \delta f$ , then it is possible to change the "colour" of the captured photons. Here we demonstrate superconducting microwave cavities, with tunable effective lengths. The tuning is obtained by varying a Josephson inductance at one end of the cavity. We show tuning by several hundred linewidths in a time  $\Delta t \ll \tau$ . Working in the few photon limit, we show that photons stored in the cavity at one frequency will leak out from the cavity with the new frequency after the detuning. The characteristics of the measured devices make them suitable for dynamic coupling of qubits.

Superconducting transmission line resonators are useful in a number of applications ranging from X-ray photon detectors [1] to parametric amplifiers [2] and quantum computation applications [3, 4, 5]. Very recently, there has been a lot of interest in tunable superconducting resonators [6, 7, 8]. In these experiments the inductive properties of the Josephson junction is implemented as a tunable element and is tuned by a bias current or a magnetic field. These devices have both large tuning ranges and high quality factors, however the speed at which these devices can be tuned has not been measured.

The interaction between a qubit and superconducting coplanar waveguide (CPW) resonator can, due to the small mode volume, be very strong when they are resonant with each other [9]. However, the interaction can be modulated, becoming weak when the qubit and the cavity are off-resonance. Taking this into account, a protocol for a controlled phase gate using two superconducting qubits and a tunable resonator was constructed by Wallquist *et al.* [10]. The advantage of using a tunable resonator for qubit interaction compared to a fixed resonator and tunable qubits is that the qubits can stay at their optimal points [11] during operation. Although a qubit design has been presented that is insensitive to charge noise [12], there is still an optimal point in the flux direction which may be essential to obtaining long coherence times. To implement the protocol suggested by Wallquist *et al.*, a CPW resonator with a large tuning range, fast tuning and high quality factor is needed. We have fabricated a quarter wavelength ( $\lambda/4$ ) CPW resonator terminated to ground via one or several Superconducting Quantum Interference Devices (SQUIDs) in series (see Fig. 1(a)). In the other end of the resonator, a small coupling capacitance is placed through which the resonator can be excited and probed using microwave reflectometry.

A SQUID can be viewed as a lumped element inductor with the nonlinear inductance

$$L_s = \frac{\Phi_0}{4\pi I_c |\cos(\pi\Phi/\Phi_0)| \sqrt{1 - \left(\frac{I}{2I_c \cos(\pi\Phi/\Phi_0)}\right)^2}} \quad (1)$$

where  $\Phi$  is the applied magnetic flux,  $\Phi_0 = \hbar/2e$  is the magnetic flux quantum,  $I_c$  is the critical current of each SQUID junction and  $I$  is the current through the SQUID. The inductance can be varied by applying a magnetic field or a bias current. When the current  $I$  is much smaller than the suppressed critical current,  $L_s$  can be considered linear. A real SQUID has also a capacitance  $C_s$  and the subgap resistance  $R_s$  in parallel with the inductance so that the total impedance of the SQUIDs is

$$Z_s = N \left( \frac{i\omega L_s R_s}{R_s + i\omega L_s - \omega^2 L_s C_s R_s} \right) \quad (2)$$

---

\*Electronic address: martins@chalmers.se

where  $N$  is the number of SQUIDs in series.

The resonator circuit can be described using the scattering matrices formulation [13] using three scattering matrixes in series. When probed with a probe voltage  $V_d$ , we find the reflection coefficient

$$\Gamma = \frac{V_r}{V_d} = \left( S_{11} + \frac{S_{12}S_{21}\Gamma_s e^{-2\gamma l}}{1 - S_{22}\Gamma_s e^{-2\gamma l}} \right). \quad (3)$$

where the  $S_{ij}$  are the scattering parameters for the coupling capacitance,  $l$  is the length of the cavity,  $\gamma = \alpha + i\beta$  is the complex wave number of the transmission line,  $\Gamma_s$  is the reflection coefficient of the SQUIDs, obtained using equation 2 as a load impedance. The parameter  $\alpha$  is the attenuation along the transmission line and for a non-tunable  $\lambda/4$  resonator  $\alpha = \pi/\lambda Q_{int}$ , where  $Q_{int}$  is the internal quality factor of the device.  $\beta = 2\pi/\lambda$ , is the phase propagation of the transmission line.

Measurements of  $\Gamma$  on two different devices are presented here. Device A has one SQUID and is tuned by an external magnetic field, while device B has six SQUIDs in series and is tuned by an on-chip flux bias (see Table I). A micrograph of a device identical to device B is showed in Fig. 1(a). Measurements of the devices were performed at the base temperature (below 20 mK) of a dilution cryostat. The measurement setup is shown in Fig. 1(b).

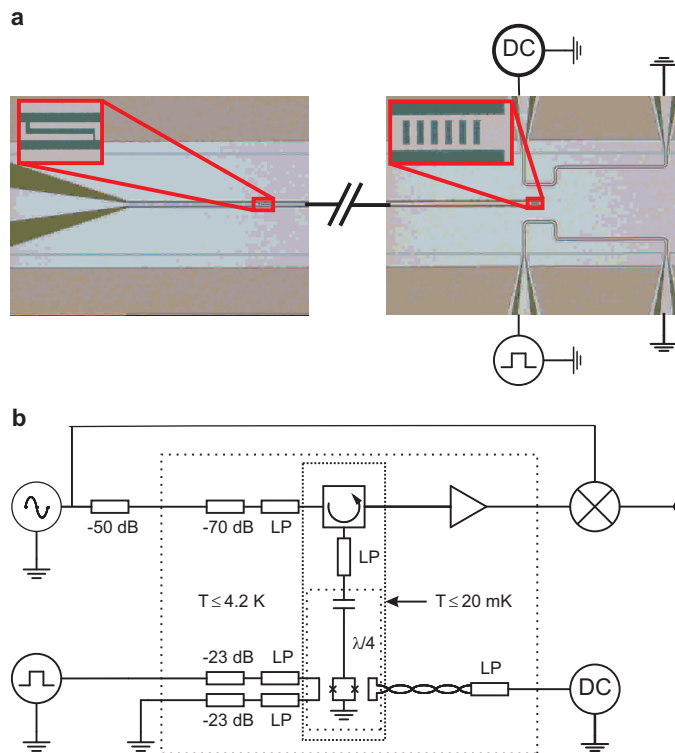


**FIG. 1: Tunable resonator and measurement setup.** **a**, A micrograph of a typical tunable  $\lambda/4$  resonator used in the experiment. The devices are fabricated on a silicon substrate with a 400 nm layer of wet-grown silicon dioxide. The cavity and the Josephson junctions forming the SQUIDs are fabricated from aluminium in a single lithography step using double angle evaporation and oxidation. The center strip is  $13 \mu\text{m}$  wide and the gaps are  $7 \mu\text{m}$ , giving a capacitance of  $170 \text{ pF/m}$  [14] and a characteristic impedance of  $50 \Omega$ . Two devices, A and B, were measured. Device B had two on-chip flux lines to tune the SQUIDs, one for DC bias and one for fast pulses, while device A could only be tuned with an external magnetic field. **b**, Schematic measurement setup. The samples are shielded from external magnetic fields using an outer Pb shield and an inner cryoperm shield. The devices are probed through a circulator placed at the base temperature of the dilution refrigerator and a HEMT amplifier with a noise temperature of 4.5 K [15] located at the 4 K stage. The excitation line has 70 dB of cold attenuation before the input port of the circulator. The fast flux line is a  $50 \Omega$  through-line going down to the chip and back to room temperature with 23 dB of attenuation in both directions. The fast flux line is filtered in both directions with 8 GHz low pass filters at the 600 mK level. The DC line has a 100 MHz low pass filter placed at 4 K. To do fast tuning measurements, the signal from the resonator is mixed with the drive signal.

Measuring the reflection coefficient as a function of applied magnetic DC field, Fig. 2(b), using a vector network

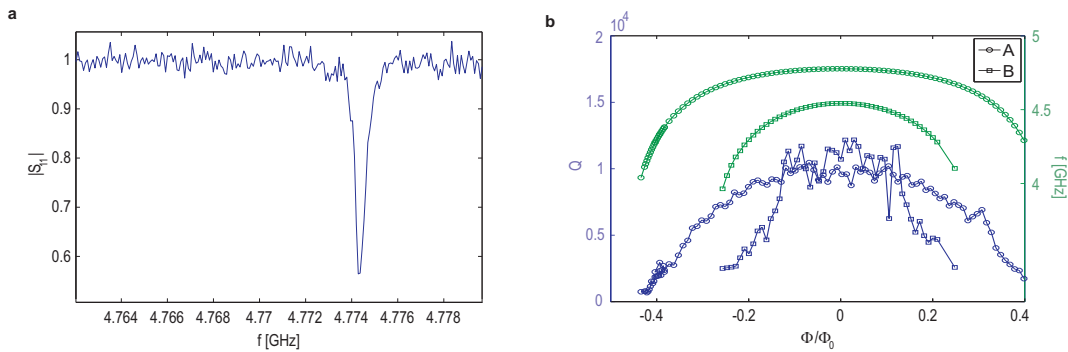


FIG. 2: **Microwave reflectometry measurements.** **a**, Magnitude of the reflection spectrum of sample A. The resonance frequency is given by the center of the dip in the spectrum and the  $Q$  value is the resonance frequency divided by the full width at half maximum. From these measurements, we can conclude that the devices are undercoupled *i.e.* the dominate source of loss is from inside the cavity and not from leakage through the coupling capacitance. The internal losses have four contributions: radiation, resistive losses in the conductor, dielectric losses, and losses in the SQUID. In the CPW design, the radiation losses are small. The resistive losses should also be small since the temperature of the device is well below the superconducting gap frequency. The losses must therefore either be due to dielectric losses or due to the SQUIDS. To address this question, a non-tunable reference device (without SQUIDS) was fabricated and measured, not shown here. The measurements showed undercoupled behaviour for this device at low drive powers, suggesting that the SQUIDS are not the limiting factor. As we increased the drive power however, the  $Q$  of the reference devices increased and we observed a transition from undercoupled to overcoupled behaviour. The power dependence seems to be consistent with what Martinis *et al.* observed for losses due to two-level fluctuators in the dielectric [16]. **b**, Resonance frequency (green) and  $Q$  value (blue) as a function of applied magnetic flux for the two devices A (circles) and B (squares). Device A has one SQUID with a critical current of  $I_c \approx 1.2 \mu\text{A}$ . Device B has six SQUIDSs in series, each with a critical current of  $I_c \approx 2.3 \mu\text{A}$ .

Sample	N	$I_c$	$f_0$	$\Delta f_{Max}$	$Q_0$	Flux bias
A	1	$1.2 \mu\text{A}$	4.77 GHz	700 MHz	10000	External
B	6	$2.3 \mu\text{A}$	4.54 GHz	480 MHz	12000	On chip

TABLE I: Parameters of the two measured devices.  $N$  is the number of SQUIDS,  $I_c$  is the critical current of the Josephson junctions,  $f_0$  is the zero flux resonance frequency,  $\Delta f_{Max}$  is the maximum detuning achieved,  $Q_0$  is the zero field  $Q$  value and the last column states how the flux bias was applied to the SQUID.

analyzer (VNA) and fitting equation 3 we get  $\alpha \sim 0.106$  dB/m and  $\beta \sim 241$  rad/m, on resonance, for sample A at zero detuning. The value of  $\beta$  on resonance gives a cavity electrical length corresponding to 86 degrees, compared to 90 degrees for a regular  $\lambda/4$  resonator. We observe a tunability  $\Delta f_{max}$  of 700 MHz for sample A and 480 MHz for sample B (see Fig. 2(b)). The  $Q$  value is obtained from the line width  $\delta f$  and depends on the detuning. Therefore, the number of detuned line widths  $\Delta f/\delta f$  as a function of detuning gives a figure of merit for the devices. This is plotted in the inset of Fig. 3(b). The maximum  $\Delta f/\delta f$  is similar for the two devices and is around 250. We observe that the  $Q$  decreases as the magnetic field is applied (see Fig. 2(b)). We do not yet understand this quantitatively. One possible reason could be inhomogenous broadening due to flux noise, but the source of this noise is not known. In particular, the typical values of  $1/f$  flux noise or  $1/f$  critical current noise are orders of magnitude smaller than needed to explain this effect.

One of the most important aspects of the device for qubit coupling is the tuning speed. A measurement of the tuning speed that relies on a change of the reflection coefficient will be limited by the ring up time of the resonator  $Q/\omega_0$ . In our case, this will be of the order of microseconds. This is however not the same as the speed at which the resonator can be tuned. If we apply fast flux pulses as we drive the resonator on resonance and mix the signal from the resonator with the drive we observe a beating between the drive frequency and the frequency of the photons leaking out of the resonator. This demonstrates that we in fact can tune the cavity much faster than the ring up time (see Fig. 3(a)).

By varying the amplitude of the flux pulse, we can map out the resonance frequency as a function of flux bias, Fig. 3(b). We can apply positive and negative flux pulses and in that way we can either increase or decrease the resonance frequency during the pulse. The leakage of energy at the detuned frequency suggests that we can both stretch and compress the photons stored in the resonator *in-situ* as we apply the flux pulse. The energy stored in the cavity on resonance can be obtained as twice the average electrical energy, and ignoring zero point fluctuations

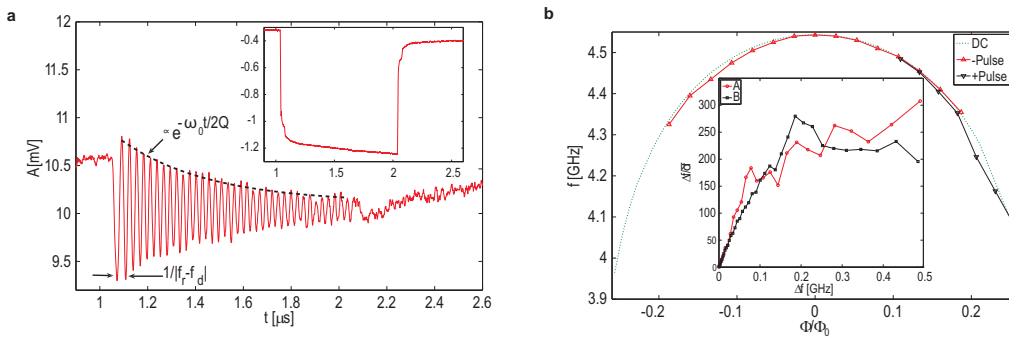


FIG. 3: **Fast detuning measurements.** **a**, To measure the tuning speed, we first drive the resonator on resonance until equilibrium is reached. A fast flux pulse is then applied to detune the resonator from the drive. We then measure the signal from the resonator as the stored energy decays. Mixing the signal with the drive frequency and filtering out the high frequency components (see Fig. 1(b) b)) we observe a decaying, oscillating signal where the frequency of the oscillations is the difference frequency of the drive and the detuned resonant frequency of the resonator. From the decay  $\tau$  of the oscillations the  $Q$  value can be obtained as  $Q = \omega\tau/2$ , where the factor of 2 is due to the fact that amplitude and not power is measured. The traces are obtained by repeatedly applying a pulse and then average the signal over several pulses. A typical number of average used is between one hundred thousand and one million. The decay measurements showed a  $Q$  of almost a factor of two less than the value obtained from line width measurements. The discrepancy can be explained by the distribution in amplitude of the applied flux pulse. As the data is average over a large number of pulses a small distribution in pulse height cause an effective increase in the decay. Inset: the pulse used to detune the resonance frequency. The amplitude of the pulse sets how far the resonator is detuned. **b**, Resonance frequency obtained from DC measurements compared to values obtained from fast pulse measurements. We can both increase and decrease the frequency with the fast pulse (indicated by up and down pointing triangles respectively) meaning that we can both stretch and compress the photons in the cavity. The inset shows how many linewidths that the devices A and B are detuned as a function of detuning.

$$E = \hbar\omega_0 N_p = 2 \int_0^l \frac{c_l V(x) V^*(x)}{2} dx \quad (4)$$

where  $V(x)$  is voltage along the transmission line and  $c_l$  is the capacitance per unit length. For the fast tuning experiment we apply a power of -141 dBm (assuming 5 dB loss in the cables) giving an average drive photon number  $N_p$  in the resonator of about 5 photons. The average number of thermal photons is much smaller than one since the temperature of the cavity is approximately 20 mK, whereas the cavity frequency corresponds to  $\sim 225$  mK. The low photon number suggest that we in fact change the frequency of individual photons as we tune the resonator with a fast flux pulse. As the cavity is detuned, the photons inside the cavity are forced to adjust to the new resonance frequency. When compressing the photons our external magnetic field is thus doing work on the photons increasing their energy.

We can obtain an estimate on how fast we can tune the device by decreasing the duration time of the flux pulse. If we apply a large detuning pulse, the observed oscillations are fast, allowing us to apply a short pulse and still observe the oscillations. In this way, we can still observe oscillations even decreasing the duration of the pulse down to a few ns. In Fig. 4 a detuning of 330 MHz for a 10 ns pulse is shown. The rise time of the flux pulse is here only about 3 ns. Due to imperfections in the fast pulse line, we get reflections (see lower inset in Fig. 4) causing a slower oscillation to occur after the fast oscillations. The pulse can be decreased even further until only one oscillation is observed (not showed here), but the duration of the flux pulse is then of the same order as the rise time.

In conclusion, we have designed and measured a tunable superconducting CPW resonator. We have demonstrated a tunability of 700 MHz for a 4.9 GHz device. As a figure of merit, we see that we can detune the devices more than 250 corrected linewidths. We have also demonstrated that our device can be tuned substantially faster than its decay time, allowing us to change the frequency of the energy stored in the cavity. Having done this in the few photon limit, we therefore assert that we can tune the frequency of individual microwave photons stored in the cavity. This can be done by several hundred MHz on the timescale of nanoseconds.

We believe that the high  $Q$  value, large tunability, and the fast tuning make this device very suitable for dynamic coupling of qubits. It should also be an interesting system for the study of fundamental physics, such as generation of nonclassical photon states [17].

Acknowledgements

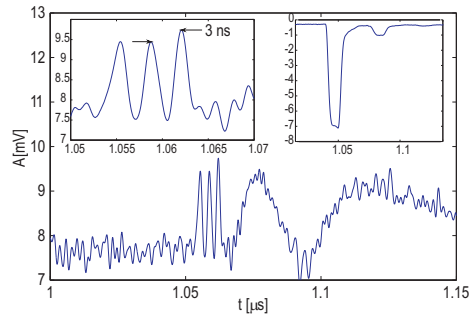


FIG. 4: **Tuning the cavity in  $\leq 10$  ns.** Signal when a 10 ns pulse is applied. The right inset shows the applied pulse. The detuning is 330 MHz, seen from the period of the oscillations (left inset). Imperfections in the bias line causes small multiple reflections of the pulse as seen in the right inset, causing the features seen after the fast oscillations in the main figure.

We acknowledge financial support from the Swedish VR and SSF, from the Wallenberg foundation and from the European Union under the EuroSQIP project. We would also like to acknowledge fruitful discussions with M. Wallquist, P. Bertet and D. Esteve.

- 
- [1] Day, P. K., LeDuc, H. G., Mazin, B. A., Vayonakis, A., and Zmuidzinas, J. *Nature* **425**(6960), 817–21 (2003).
  - [2] Tholen, E. A., Ergul, A., Doherty, E. M., Weber, F. M., Gregis, F., and Haviland, D. B. *Applied Physics Letters* **90**(25) (2007).
  - [3] Wallraff, A., Schuster, D. I., Blais, A., Frunzlo, L., Huang, R. S., Majer, J., Kumar, S., Girvin, S. M., and Schoelkopf, R. J. *Nature* **431**(7005), 162–7 (2004).
  - [4] Majer, J., Chow, J. M., Gambetta, J. M., Koch, J., Johnson, B. R., Schreier, J. A., Frunzio, L., Schuster, D. I., Houck, A. A., Wallraff, A., Blais, A., Devoret, M. H., Girvin, S. M., and Schoelkopf, R. J. *Nature* **449**(7161), 443–447 (2007).
  - [5] Sillanpaa, M. A., Park, J. I., and Simmonds, R. W. *Nature* **449**(7161), 438–442 (2007).
  - [6] Osborn, K. D., Strong, J. A., Sirois, A. J., and Simmonds, R. W. *IEEE Transactions on Applied Superconductivity* **17**(2), 166–8 (2007).
  - [7] Castellanos, M. A. and Lehnert, K. W. *Applied Physics Letters* **91**, 083509–1 (2007).
  - [8] Placios-Laloy, A., Nguyen, F., Mallet, F., Bertet, P., Vion, D., and Esteve, D. *To be published* (2007).
  - [9] Blais, A., Ren-Shou, H., Wallraff, A., Girvin, S. M., and Schoelkopf, R. J. *Physical Review A (Atomic, Molecular, and Optical Physics)* **69**(6), 62320–1 (2004).
  - [10] Wallquist, M., Shumeiko, V. S., and Wendin, G. *Physical Review B (Condensed Matter and Materials Physics)* **74**(22), 224506–1 (2006).
  - [11] Vion, D., Aassime, A., Cottet, A., Joyez, P., Pothier, H., Urbina, C., Esteve, D., and Devoret, M. H. *Science* **296**(5569), 886–889 (2002).
  - [12] Koch, J., Yu, T. M., Gambetta, J., Houck, A. A., Schuster, D. I., Majer, J., Blais, A., Devoret, M. H., Girvin, S. M., and Schoelkopf, R. J. *Physical Review A - Atomic, Molecular, and Optical Physics* **76**(4) (2007).
  - [13] Collin. *Foundations for microwave engineering*. McGraw-Hill, international edition edition, (1992).
  - [14] Gevorgian, S., Linner, L. J. P., and Kollberg, E. L. *IEEE Transactions on Microwave Theory and Techniques* **43**(4), 772–9 (1995).
  - [15] Chincarini, A., Gemme, G., Iannuzzi, M., Parodi, R., and Vaccarone, R. *Classical and Quantum Gravity* **23**(8), 293–8 (2006).
  - [16] Martinis, J. M., Cooper, K. B., McDermott, R., Steffen, M., Ansmann, M., Osborn, K. D., Cicak, K., Seongshik, O., Pappas, D. P., Simmonds, R. W., and Yu, C. C. *Physical Review Letters* **95**(21), 210503–1 (2005).
  - [17] Agarwal, G. S. and Arun Kumar, S. *Physical Review Letters* **67**(26), 3665–8 (1991).